Rate of Quantal Transmitter Release at the Mammalian Rod Synapse

Rukmini Rao,*‡ Gershon Buchsbaum,* and Peter Sterling‡
Departments of *Bioengineering and ‡Neuroscience, University of Pennsylvania, Philadelphia, Pennsylvania 19104 USA

ABSTRACT Under scotopic conditions, the mammalian rod encodes either one photon or none within its integration time. Consequently the signal presented to its synaptic terminal is binary. The synapse has a single active zone that releases neurotransmitter quanta tonically in darkness and pauses briefly in response to a rhodopsin isomerization by a photon. We asked: what minimum tonic rate would allow the postsynaptic bipolar cell to distinguish this pause from an extra-long interval between quanta due to the stochastic timing of release? The answer required a model of the circuit that included the rod convergence onto the bipolar cell and the bipolar cell's signal-to-noise ratio. Calculations from the model suggest that tonic release must be at least 40 quanta/s. This tonic rate is much higher than at conventional synapses where reliability is achieved by employing multiple active zones. The rod's synaptic mechanism makes efficient use of space, which in the retina is at a premium.

INTRODUCTION

The spatio-temporal density of photons striking the retina in deep twilight is quite modest, on the order of 10 photons/μm^2/s. With nightfall this flux drops by three orders of magnitude, so that in starlight there are only 10^{-2} photons/μm^2/s (Sterling et al., 1987). The mammalian rod has a small cross-sectional area ($\sim$3 μm^2) and a modest integration time ($\sim$250 ms; Baylor et al., 1984; Nakatani et al., 1991); it absorbs 33% of the incident photons, of which half produce a rod response. Consequently, between starlight and twilight, the individual rod signals either one photon or none (Sterling et al., 1987; MacLeod et al., 1989). Although mammalian rods are not coupled to each other by gap junctions, they are coupled to cones (Kolb, 1977; Smith et al., 1986). However, calculations suggest that, when there is less than 1 photon/rod/integration time, the rod-cone junctions uncouple to isolate the rod (Smith et al., 1986). Thus, the signal reaching the synapse of a mammalian rod is binary: one photon or none.

Several lines of evidence suggest that this binary signal is transferred reliably. First, there is evidence that humans can actually detect single photon events (Sakitt, 1972). Second, cat ganglion cells in dim light show small bursts (2 or 3 spikes) apparently corresponding to a single photoisomerization, the isomerization of a rhodopsin molecule (Rh*) by a single photon (Barlow et al., 1971; Mastronarde, 1983). Similar bursts continue in the dark, apparently triggered by single, thermal isomerizations of rhodopsin. In fact, the ganglion cell's dark firing rate (18 spikes/s) seems to be accounted for by the rate of thermal isomerization per rod times the number of rods converging on the ganglion cell (0.006 Rh*/rod/s $\times$ 1000 rods/ganglion cell $\times$ 3 spikes/Rh*; Barlow et al., 1971; Mastronarde, 1983; Sterling et al., 1988). Thus, the Rh* signal, whether triggered by light or heat, traverses not only the rod synapse, but a whole chain of subsequent synapses to reach the ganglion cell and then the brain.

Because the mechanism employed to transmit the binary signal (0 or 1 Rh*) is stochastic, we wondered how it could achieve the requisite reliability. At the rod synapse, a single "active zone" (region of vesicle exocytosis) releases transmitter quanta continuously in darkness (signaling 0) and pauses briefly following an Rh* event (signaling 1). Since the interval between successive quanta in darkness varies stochastically, an extra-long interval could be mistaken for the pause in tonic release that signifies an Rh* event. Thus, the resulting signal to the brain would be falsely positive. Consequently, the question regarding reliability is well defined: what rate of tonic release insures that the interval between quanta is rarely long enough to elicit a false positive? Clearly, a higher tonic rate would produce fewer extra-long intervals and thus fewer errors. Here, we compute the maximum interquantal interval that can be tolerated before a false positive occurs. This interval and the statistics of quantal release provide a numerical estimate for the minimum tonic rate required at the rod synapse.

MODEL

Fig. 1 shows the early stages of the mammalian rod circuit. In darkness, the rod voltage fluctuates about a level of depolarization that promotes tonic release of transmitter (Trifonov, 1968; Dowling and Ripps, 1973; Cervetto and Piccolino, 1974; Kaneko, 1979; Detwiler et al., 1984). An Rh*, hyperpolarizing the rod and suppressing transmitter release, depolarizes the bipolar cell (Dacheux and Raviola, 1986). We assume that the bipolar cell releases no transmitter in darkness but, when depolarized beyond some threshold, releases transmitter in a brief burst onto neurons at the next stage of the pathway. This shower of quanta transfers the Rh* signal.

Thus, the rod synapse must accomplish two critical tasks. First, it must minimize the number of false negatives; i.e., ensure in the presence of a true Rh* that the pause in transmitter release is long enough for the bipolar cell to depolarize

Received for publication 20 October 1993 and in final form 21 April 1994.
Address reprint requests to Dr. Rukmini Rao, Department of Neuroscience, 123 Anatomy/Chemistry Building, University of Pennsylvania Medical Center, Philadelphia, PA 19104. Tel.: 215–898–7536; Fax: 215–898–9871; E-mail: rukki@retina.anatomy.upenn.edu.

0006-3495/94/07/57/07 $2.00

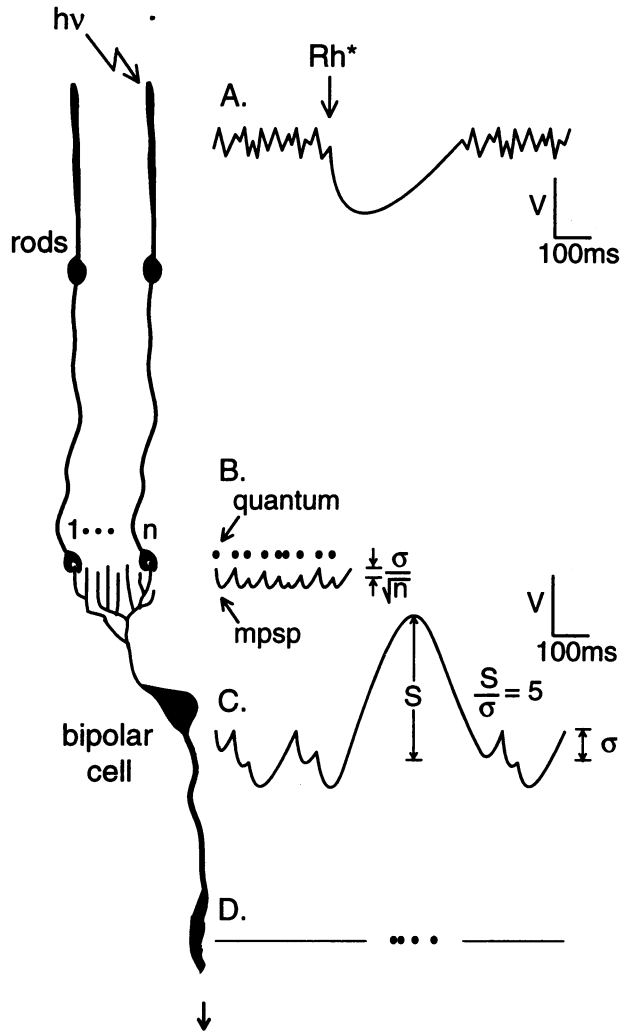

FIGURE 1 *Left:* Early stages of rod circuit in cat retina (Boycott and Kolb, 1973; Freed et al., 1987; Sterling et al., 1988): *n* rods converge onto a bipolar cell, each contacting a separate dendrite. *Right:* Physiological sequence triggered by a photon ($h\nu$) absorption. (*A*) Diagram of the rod voltage response: an absorbed photon isomerizes a rhodopsin molecule (Rh*) leading to a prolonged, all-or-none, hyperpolarizing response (Baylor et al., 1984). (*B*) Diagram of the tonic quantal release at a rod terminal (each dot indicates a quantum) and the response of the postsynaptic bipolar dendrite: each quantum evokes an mpsp. We note that the response termed here "mpsp" is actually just the tip of the full mpsp. This fact does not affect the rationale to compute the tonic dark rate. However, it does imply that an Rh* signal increases the mean bipolar voltage by the amplitude of the full mpsp, not just the amplitude of its tip. (*C*) Diagram of the response at the bipolar soma: the noise (σ) reflects temporal integration of mpsp's from *n* rods with each rod contributing $\sigma/n^{1/2}$; an Rh* in one rod suppresses its tonic release, causing depolarization of amplitude *S* in the bipolar cell. (*D*) Diagram of the quantal release at the bipolar axon: depolarization of the bipolar cell by an Rh* event triggers a brief period of transmitter release. The circuit shown here for cat is highly conserved across mammalian species, including human (Kolb et al., 1992), monkey (Grünert and Martin, 1991), rabbit (Vaney et al., 1991), and rat (Chun et al., 1993).

to its threshold. Second, it must minimize the number of false positives; i.e., ensure in the absence of a true Rh* that the interval between quanta is rarely long enough for the bipolar cell to reach threshold. Since the first task concerns the response of the rod synapse to light, it does not enter the present calculation which concerns only the tonic rate of transmitter release in darkness.

The probability that a bipolar cell signals a false positive to the next stage depends on its signal-to-noise ratio (S/σ). For a $S/\sigma = 5$ in the bipolar cell, the probability of false positives is ~0.01. If S/σ is halved, the false positive probability rises sharply to ~0.11, and if S/σ is doubled, the false positive probability plummets to $\sim 4 \times 10^{-7}$ (see Appendix for these calculations). Since the rod reliably encodes an Rh* event using $S/\sigma \sim 5$ (Baylor et al., 1984), little would be achieved by making the bipolar cell more accurate. Therefore, the model assumes that $S/\sigma = 5$ in the bipolar cell and hence that the probability of false positives is 0.01.

The bipolar cell's noise (σ) we attribute to voltage fluctuations due to tonic synaptic input. The bipolar dendritic arbor resembles a candelabra with one rod synapse at the tip of each terminal dendritic segment. Voltage fluctuations evoked at the *n* rod synapses sum linearly at the bipolar soma. Thus, the noise contributed by each dendritic terminal is $\sigma/n^{1/2}$.

At a given dendritic terminal, the postsynaptic potential (mpsp) evoked by a single transmitter quantum is assumed to be an all-or-none shot event, i.e., of constant amplitude, shape, and duration (Redman, 1990; Larkman et al., 1991) (Fig. 1, *B*). It is further assumed that the hyperpolarization caused by one quantum is maximal for that synapse and that successive quanta, no matter how closely spaced temporally, evoke no greater hyperpolarization. Supporting this assumption is evidence at central synapses that one quantum saturates all the postsynaptic receptors (Jack et al., 1981; Edwards et al., 1990; Tong and Jahr, 1994). Thus, the model attributes fluctuation in dendritic voltage solely to differences in the time interval between successive quanta. The problem then is to calculate how long this interval can be before the dendritic voltage depolarizes beyond $\sigma/n^{1/2}$.

This calculation depends on the time course of the mpsp. This is unknown but was estimated as follows (Fig. 2 *A*). We based the shape of the mpsp on that calculated for the "unitary event" underlying the noise spectrum of the turtle bipolar cell (Ashmore and Copenhagen, 1980):

$$a(t) = \frac{\alpha t}{t_p} \exp(-t/t_p + 1) \qquad (1)$$

where $a(t)$ is the voltage, α is the peak amplitude, and t_p is the time to peak. The time course of the mpsp can be considered as two intervals: τ, the half-width of the mpsp, and γ, the time required for the decaying mpsp to depolarize the dendrite by $\sigma/n^{1/2}$ from its half-maximum level. We first estimated γ and then used it to estimate τ.

γ describes the decay (depolarizing) phase of the bipolar mpsp. This phase represents the commencement of the Rh* signal in the bipolar cell, so γ can be measured from the bipolar cell's depolarizing response to a light step. Fig. 2 *A* (*right*) shows this response for a rabbit rod bipolar cell at 35°C (taken from Dacheux and Raviola, 1986). The rise in response to the onset of the light step is equivalent to the rise of a flash response to 500 Rh*/bipolar cell. We assume that

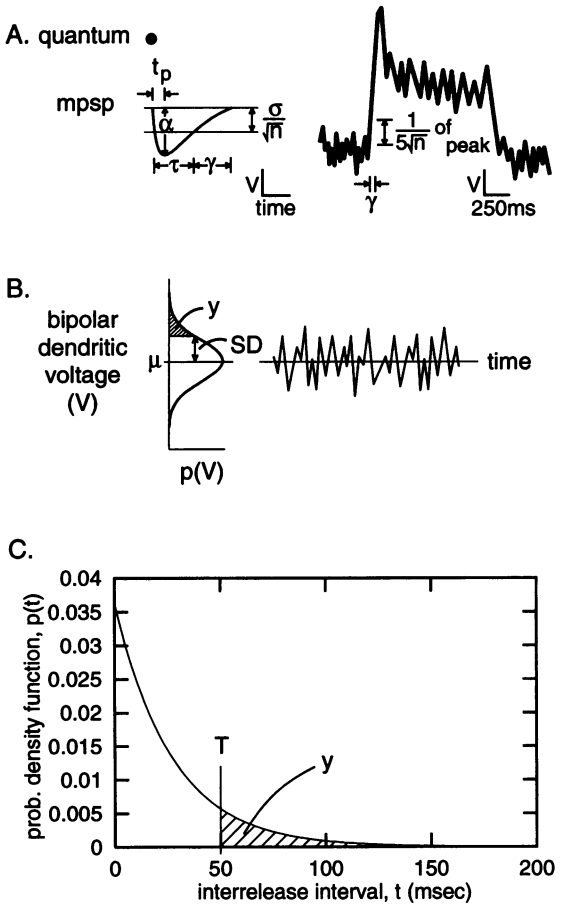

FIGURE 2 (*A*) *Left:* Shape of the mpsp, with a peak amplitude of α and a time to peak of t_p, plotted according to Eq. 1. The equation describes the voltage as asymptoting to the initial voltage; however, we allow the mpsp to depolarize past the initial voltage using the slope of the curve at one-quarter amplitude. The mpsp's time course can be considered as two intervals: τ, the half-width, and γ, the time required for the decaying mpsp to depolarize the dendrite by $\sigma/n^{1/2}$ from its half-maximum level. *Right:* Rabbit rod bipolar response to a light step (redrawn from Fig. 7 in Dacheux and Raviola, 1986). γ is the time for the response voltage to rise to $1/5n^{1/2}$ of the peak amplitude. (*B*) Given that the bipolar dendritic voltage in the absence of an Rh* has a Gaussian distribution ($\mu \pm$ SD) with SD = $\sigma/n^{1/2}$, y is the area under the curve greater than μ + SD (hatched), divided by the total area under the curve; thus, $y \sim 0.16$. (*C*) Probability density function of interrelease intervals, $p(t)$, for a Poisson release process. This plot is such that when the maximum interval (T) between quanta is 50 ms, the probability (y) of exceeding it (the hatched area under the curve as a fraction of the total area) is ~0.16. The mean release rate required to produce this plot is 37 quanta/s.

the time to peak for this response is the mean time to peak for the underlying 1 Rh* responses. Thus, the time (γ) required for a bipolar dendrite to depolarize from its mean level by $\sigma/n^{1/2}$, i.e., by $S/5n^{1/2}$ given $S/\sigma \sim 5$, is the time required for this response voltage to rise to $1/5n^{1/2}$ of the peak amplitude. To determine τ, the half-width of the mpsp, we normalized the mpsp's peak amplitude (α) to one and adjusted the time to peak (t_p) until the time to depolarize from half-maximum to the initial level equaled γ (see Eq. 1). This set the time course of the mpsp and hence, its half-width, τ.

By our definition, τ plus γ gives T, the entire temporal extent of the bipolar mpsp. This is the maximum time between quanta before the bipolar dendritic voltage depolarizes beyond $\sigma/n^{1/2}$. Thus, the question now becomes: given that release is stochastic, what minimum tonic rate would ensure intervals between quanta that are rarely longer than T?

"Rarely" implies some low probability (y) that the bipolar dendritic voltage does depolarize beyond $\sigma/n^{1/2}$. We assume the bipolar dendritic voltage in darkness to be well approximated by a Gaussian distribution (as depicted in Fig. 2 *B*). Then, with a standard deviation (SD) of $\sigma/n^{1/2}$, y is the area under the curve greater than the mean plus the standard deviation (hatched region) divided by the total area under the curve. Our assumption that the mpsp is of maximal amplitude implies truncation of the Gaussian's lower tail. However, the area under this tail adds to the probability near the maximum amplitude and thus does not affect the value for y. Consequently, y is ~0.16 and the next task is to calculate what minimum tonic rate ensures that intervals between quanta exceed T with a probability of only 16%.

We modeled quantal release as a Poisson process. At the mammalian rod synapse, the binomial statistics of transmitter release can be approximated as Poisson because, at the single active zone, the number of vesicle release sites is apparently large and the probability of release per site is low (Rao and Sterling, 1991). Poisson statistics imply that the probability density function describing intervals between quanta is exponential:

$$p(t) = \rho \exp(-\rho t) \tag{2}$$

where t is the interval between quanta and ρ is the quantal release rate. The decay of this distribution, plotted in Fig. 2 *C*, depends only on the release rate. When the maximum interval between quanta is T, and the probability of exceeding it is y (hatched region), the distribution is specified; hence, so is the quantal release rate that produces it. In other words, we solve

$$y = \int_T^\infty p(t)\, dt \tag{3}$$

substituting $p(t)$ from Eq. 2 to obtain

$$\rho = -\frac{\ln y}{T} \tag{4}$$

RESULTS

Fig. 2 *C* plots the probability density function for intervals between rod quanta in cat, where the rod-to-bipolar cell convergence (n) is 20. For an mpsp temporal extent (T) of 50 ms, the minimum tonic release rate is 37 quanta/s. If the mpsp is shorter or longer (T = 25, 75 ms), the minimum tonic rates are, respectively, 74 and 25 quanta/s (marked in Fig. 3 *A*). The minimum tonic rate also depends on the specified S/σ, and Fig. 3 *A* shows the linearity of this relationship. However, the dependence of the false positive probability on S/σ is not linear (see Appendix and Fig. 4 *E*), so an increase in tonic rate from 37 to just 47 quanta/s would cut the false

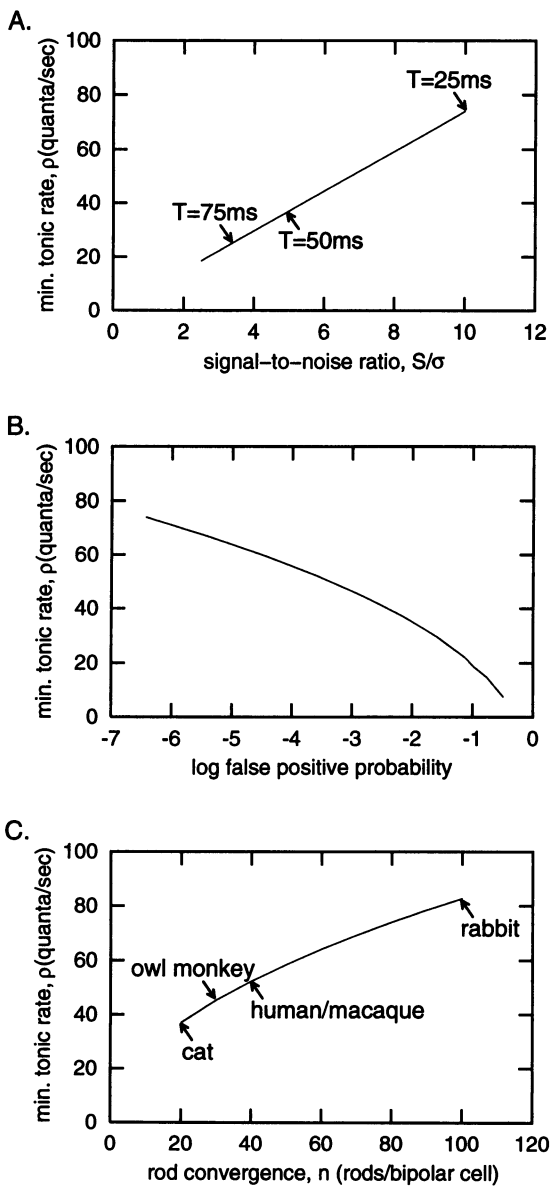

FIGURE 3 (*A*) Plot of minimum tonic rate (ρ) vs. S/σ: the rate is directly proportional to signal-to-noise ratio. Rates for T = 25, 50, and 75 ms are 74, 37, and 25 quanta/s, respectively. (*B*) Plot of ρ vs. the log false positive probability. (*C*) Plot of ρ vs. convergence (n): the rate is proportional to the square root of the convergence. Arrows mark the values for cat, owl monkey, human, macaque, and rabbit.

positive probability by 10-fold (Fig. 3 *B*). Thus, the incremental cost of increased reliability is modest.

The rod convergence varies between species: 20 rods/bipolar cell in cat (Boycott and Kolb, 1973; Freed et al., 1987), 30 in owl monkey (Ogden, 1975), 20–60 in macaque (Boycott and Dowling, 1969; Kolb, 1970; Grünert and Martin, 1991), 30–45 in human (Kolb et al., 1992), and up to 100 in rabbit (Dacheux and Raviola, 1986; Young and Vaney, 1991). Greater convergence increases noise in the bipolar cell by $n^{1/2}$ (Freed et al., 1987). Thus, to maintain the same degree of reliability, i.e., to constrain the noise in the bipolar cell to σ, greater convergence would require a higher tonic release rate. The relation is such that a fivefold difference in convergence (cat vs. rabbit) would require roughly doubling the rod's minimum tonic rate (Fig. 3 *C*).

DISCUSSION

For different assumptions regarding the temporal extent of the bipolar mpsp, the minimum tonic rate calculated for the rod synapse is within twofold of 40 quanta/s. For different assumptions regarding the reliability of transmission (probability of false positives), the calculations show that the incremental cost of increasing reliability from a false positive probability of 0.01 to 0.001, is small (~25%). Thus, the minimum tonic rate calculated here is realistic to within a factor of two.

If the true shape of the mpsp differs from that assumed, voltage at the bipolar soma would appear different. However, the mpsp shape was used merely to obtain a value for temporal extent; therefore, if that parameter remains constant, a different shape would not affect the calculation of rate. On the other hand, if the mpsp is not a shot event (as assumed) but rather varies in amplitude, the minimum tonic rate would be higher. Thus, the values we have calculated should be considered lower bounds. The actual rate may eventually be measured directly by electrical (von Gersdorff and Matthews, 1994) or optical (Betz and Bewick, 1993) recordings.

A quantal rate for the rod was first estimated by Falk and Fatt (1974) and suggested to be more than 10 times the value derived here. Their calculation depended, not on the release statistics, but rather on the ratio of the bipolar cell conductance to the quantal conductance. In retrospect, their estimate of the whole cell conductance at 10^{-6}mho (10^{-6}S) was probably too high, and their calculation of quantal conductance (derived from the frog miniature endplate potential) assumed an mpsp that decayed 10 times faster than estimated here. Thus, if their calculations used parameter values that we now believe are more reasonable, the two quite different models would give similar results.

Differences between mammals

The rod circuit, though conserved in basic plan across mammalian species, varies quantitatively. As noted, convergence at the first stage, rod-to-bipolar cell, can differ by fivefold (n = 100 in rabbit vs. n = 20 in cat). Convergence at this stage represents only a small fraction of the total convergence onto the ganglion cell (Freed et al., 1987; Sterling et al., 1988); therefore, differences at this stage are probably unrelated to acuity. More likely, the variation corresponds to the efficiency with which the eye of a given species collects sparse photons. For example, the rabbit eye, lacking the cat's tapetum and having a smaller pupil, probably collects fewer photons for a given luminance. Thus, the rabbit bipolar cell can sustain greater convergence for the same dynamic range.

One obvious advantage of matching convergence to light-gathering capacity is that space is saved. Thus, corresponding to the fivefold greater convergence (rabbit vs. cat) is a sevenfold lesser density of rod bipolar cells (6000/mm^2 in rabbit

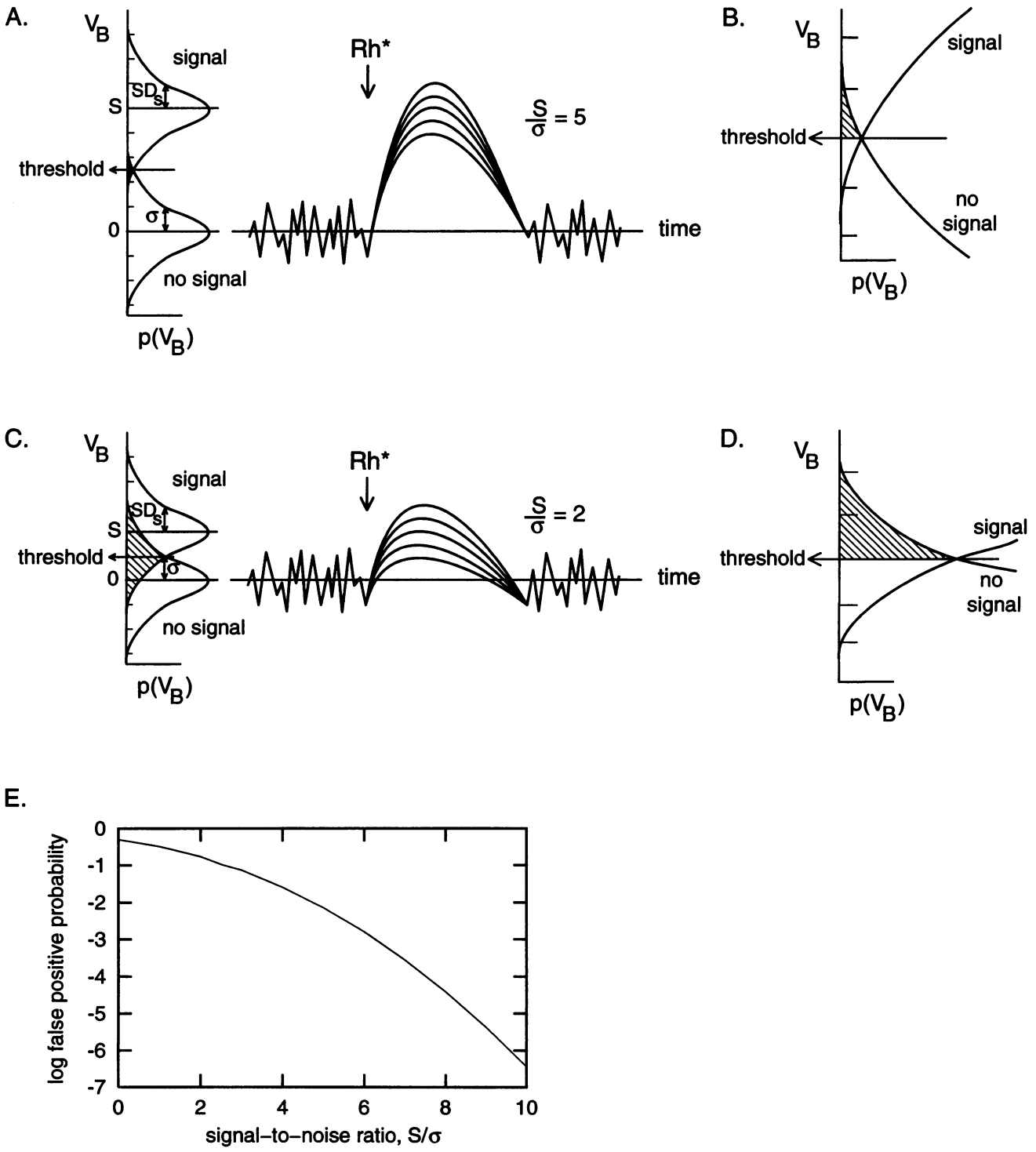

FIGURE 4 (*A* and *C*) *Right:* Hypothetical voltage responses, V_B, of a rod bipolar cell to an Rh* event. *Left:* Gaussian probability distributions of the voltage, $p(V_B)$, with and without a signal. We take the "no signal" distribution to have mean and standard deviation, $0 \pm \sigma$, and the "signal" distribution to have mean and standard deviation, $S \pm SD_S$. Since $\sigma = SD_S$, the widths of the distributions are equal and the threshold can be set halfway in between. (*A*) $S/\sigma = 5$. (*C*) $S/\sigma = 2$. (*B* and *D*) Higher magnifications of (*A*) and (*C*), respectively, showing the regions where the two distributions overlap. (*E*) Plot of log false positive probability vs. S/σ.

(Young and Vaney, 1991) vs. 40,000/mm^2 in cat (Freed et al., 1987)). Since the rabbit rod bipolar cell is somewhat larger than the cat's, the total volume of retina devoted to the rod bipolar cell array in rabbit is only about two-thirds that of cat. The rabbit's retina over the span of the bipolar cell (outer plexiform through inner plexiform layers) is about 17 μm thinner than the cat's, and about 20% of this difference is attributable to the difference in volume of the rod bipolar array.

These calculations show the relation of a fundamental cellular mechanism (transmitter release) to the design of a neural circuit (rod convergence and bipolar density) and ultimately to the macroscopic structure of the tissue (retinal thickness). If tonic rate at the rod synapse is raised, or a greater probability of false positives is tolerated, rod convergence can be increased, bipolar cells decreased, etc. Such matching of design across levels of organization, termed "symmorphosis," is well known for somatic structure-function relationships (Weibel et al., 1991; Diamond, 1993) but this may be the first example at the level of a neural circuit.

Comparison to other synapses

A tonic rate on the order of 40 quanta/s is considerably higher than observed at the active zones of "conventional" (non-ribbon) synapses. A single conventional active zone releases one quantum per action potential with a probability less than one (Korn and Faber, 1991). At the frog neuromuscular junction, tonic stimulation at 40 Hz releases less than 40 quanta/active zone/s, and even this decays sharply over the first minute (Betz and Bewick, 1993). Application of α-latrotoxin to this neuromuscular junction at low temperature raises sustained release to 0.25 quanta/active zone/s (assuming ~400 active zones; Heuser et al., 1979) for only 2 h (Ceccarelli et al., 1988). At room temperature, the rate increases by an order of magnitude, but the duration declines proportionately. At the crab T-fiber synapse, tonic presynaptic depolarization releases an estimated 60–120 quanta/s at one active zone, but the rate declines after only 2 s (J.-W. Lin, personal communication).

Another example, from the retina itself, concerns the conventional synapses between amacrine neurons. In cultured chick amacrine cells, an upper bound to the release rate at an active zone is estimated at 19–42 quanta/s (Gleason et al., 1993). However, this calculation assumes that the release probability at an active zone is 1. Therefore, it may underestimate the number of active zones forming the junction and thus overestimate the peak rate. Further, although this rate is sustained over hundreds of milliseconds, it declines over 10 stimulus trials spaced 4 s apart. Therefore, whatever the true peak rate at the amacrine active zone, it is not sustained for very long. Similarly, the giant axon terminal of the goldfish bipolar cell may release as many as 200 quanta/active zone/s but this rate declines sharply after 2 ms (von Gersdorff and Matthews, 1994).

On the other hand, the rate sustained at the large ribbon active zones in turtle cone seems remarkably similar to the rate we have calculated here. Analyzing the noise spectrum of the hyperpolarizing cone bipolar cell in darkness, Ashmore and Copenhagen (1983) calculated 9200 "elementary transmitter events" per second. This rate they divided by the estimated number of active zones contacting the bipolar cell, to arrive at a tonic rate of 20 quanta/s. Thus, the capacity to secrete quanta at a high rate for long periods may be conserved across vertebrate photoreceptors.

Functional architecture at rod terminal

The need to sustain a high tonic rate may explain the unique architecture of the rod active zone. Sustained quantal release implies: 1) a substantial number of vesicle docking sites; 2) a mechanism for their prompt reloading; 3) a handy depot of fresh vesicles. The rod's vesicle-docking region is linear and extensive, with room for 100–150 vesicles (Rao and Sterling, 1991) (vs. ~20 at a conventional retinal synapse; Raviola and Raviola, 1982). The obvious candidate for a resupply depot is the plate-like synaptic ribbon to which 500–600 vesicles are attached (Rao and Sterling, 1991). The ribbon's basal edge anchors parallel to the docking region at a distance of 30 nm. Since this is about the diameter of one vesicle, the arrangement minimizes the distance for translocation of a vesicle to resupply an empty docking site.

Although most neurons transfer a signal by employing a low quantal rate at multiple active zones (see above), the rod employs a high rate at a single active zone. This design conserves space. For example, the cone terminal with 17 active zones (Sterling and Harkins, 1990) occupies ~8 times the volume of the rod terminal. Rods are the most numerous of retinal neurons (in cat, up to 460,000/mm^2; Steinberg et al., 1973) and their terminals occupy 66% of the retinal volume devoted to photoreceptor terminals. Yet, rods are the most impoverished of signal: a rod in starlight absorbs a photon only about once in 10 min (Sterling et al., 1987; MacLeod et al., 1989). Therefore, the single active zone with a high quantal rate may reflect pressure to "miniaturize" the apparatus needed for the reliable transfer of a binary signal.

We are grateful for many helpful comments on an early draft of this paper by Drs. Noga Vardi, Robert G. Smith, Donald S. Faber, David Copenhagen, Ann Stuart, Geoffrey Gold, Jen-Wei Lin, and Michael Freed.
This work was supported by National Eye Institute grants EY00828 and EY08124.

APPENDIX

Dependence of the false positive probability on S/σ

Barlow pointed out the relationship between the probability of errors and the S/σ of a system (Barlow, 1985). To calculate the probability of false positives from the S/σ, we first define a voltage threshold such that bipolar cell voltages above this threshold indicate an Rh* signal, while those below this threshold indicate no Rh* signal. Then, we calculate the probability that, for any given observation, the bipolar cell voltage in the absence of an Rh* signal exceeds this threshold and indicates an Rh* signal (i.e., a false positive). This probability indicates the fraction of outputs that signal the presence of an input event although the input event is absent. We use "probability of false positives" in the context of signal detection theory, where it is also known as the probability of false alarms (van Trees, 1968).

Consider the bipolar cell response to an Rh* for different signal-to-noise ratios. The Gaussian probability distributions of voltages, $p(V_B)$, with and without an Rh* signal are shown at the left margin of Fig. 4, *A* and *C*. The "no signal" distribution we take to have a mean of 0 and a SD of σ; the "signal" distribution then has a mean of S and a SD of SD_S. Since variance of the voltage with or without a signal is evoked by transmitter release from, respectively, $n - 1$ or n rods, the mechanism producing the standard deviation in both cases is essentially the same. Thus, we take $\sigma = SD_S$. Then the two distributions are of equal width, so we take the threshold to be set equidistant from their peaks. In other words, a bipolar voltage lying below this level indicates "no signal" and a voltage lying above it indicates "signal."

The overlap of the two distributions is set by the signal-to-noise ratio (S/σ). For example, $S/\sigma = 5$ (Fig. 4 *A*) leads to less overlap than the distributions with $S/\sigma = 2$ (Fig. 4 *C*). The area of overlap (hatched regions in

Fig. 4, *A* and *C*) indicates the probability that a given bipolar voltage will lead to an incorrect signal, i.e., that a voltage exceeding threshold and thus indicating a signal will result without a signal (false positive) or a voltage lying below threshold and thus indicating no signal will result with a signal (false negative). This area of overlap divided by the sum of the areas under the two distributions gives the probability of errors. This probability is 0.01 for $S/\sigma = 5$ and 0.17 for $S/\sigma = 2$.

From the same plots, we calculate the probability of false positives, i.e., the probability that, without an Rh* event, bipolar voltage exceeds threshold and thus indicates an Rh*. This probability is the hatched area in Fig. 4, *B* and *D* divided by the area under the "no signal" distribution *alone*. Thus, for $S/\sigma = 5$, the false positive probability is 0.01 and, for $S/\sigma = 2$, it is 0.17. Fig. 4 *E* shows the false positive probability as a function of S/σ.

REFERENCES

Ashmore, J. F., and D. R. Copenhagen. 1980. Different postsynaptic events in two types of retinal bipolar cell. *Nature*. 287:84–86.

Ashmore, J. F., and D. R. Copenhagen. 1983. An analysis of transmission from cones to hyperpolarizing bipolar cells in the retina of the turtle. *J. Physiol.* 340:569–597.

Barlow, H. B. 1985. General principles: the senses considered as physical instruments. *In* Cambridge Texts in the Physiological Sciences 3. The Senses. H. B. Barlow and J. D. Mollon, editors. Cambridge University Press, Cambridge, England. 1–33.

Barlow, H. B., W. R. Levick, and M. Yoon. 1971. Responses to single quanta of light in retinal ganglion cells of the cat. *Vision Res.* S3:87–101.

Baylor, D. A., B. J. Nunn, and J. L. Schnapf. 1984. The photocurrent, noise and spectral sensitivity of rods of the monkey *Macaca fascicularis*. *J. Physiol.* 357:575–607.

Betz, W. J., and G. S. Bewick. 1993. Optical monitoring of transmitter release and synaptic vesicle recycling at the frog neuromuscular junction. *J. Physiol.* 460:287–309.

Boycott, B. B., and J. E. Dowling. 1969. Organization of the primate retina: light microscopy. *Phil. Trans. Roy. Soc. (London) B*. 255:109–184.

Boycott, B. B., and H. Kolb. 1973. The connections between bipolar cells and photoreceptors in the retina of the domestic cat. *J. Comp. Neurol.* 148:91–114.

Ceccarelli, B., W. P. Hurlbut, and N. Iezzi. 1988. Effect of α-latrotoxin on the frog neuromuscular junction at low temperature. *J. Physiol.* 402: 195–217.

Cervetto, L., and M. Piccolino. 1974. Synaptic transmission between photoreceptors and horizontal cells in the turtle retina. *Science*. 183:417–419.

Chun, M. H., S. H. Han, J. W. Chung, and H. Wässle. 1993. Electron-microscopic analysis of the rod pathway of the rat retina. *J. Comp. Neurol.* 332:421–432.

Dacheux, R. F., and E. Raviola. 1986. The rod pathway in the rabbit retina: a depolarizing bipolar and amacrine cell. *J. Neurosci.* 6:331–345.

Detwiler, P. B., A. L. Hodgkin, and T. D. Lamb. 1984. A note on the synaptic events in hyperpolarizing bipolar cells of the turtle's retina. *In* Photoreceptors. A. Borsellino and L. Cervetto, editors. Plenum Publishing Corp., New York. 285–293.

Diamond, J. 1993. Evolutionary physiology. *In* The Logic of Life: the Challenge of Integrative Physiology. C. A. R. Boyd and D. Noble, editors. Oxford University Press, New York. 89–111.

Dowling, J. E., and H. Ripps. 1973. Effect of magnesium on horizontal cell activity in the skate retina. *Nature*. 242:101–103.

Edwards, F. A., A. Konnerth, and B. Sakmann. 1990. Quantal analysis of inhibitory synaptic transmission in dentate gyrus of rat hippocampal slices: a patch clamp study. *J. Physiol.* 430:213–240.

Falk, G., and P. Fatt. 1974. Limitations to single-photon sensitivity in vision. *In* Lecture Notes in Biomathematics, Vol. 4: Physics and Mathematics of the Nervous System. M. Conrad, W. Gittinger, and M. Dal Cin, editors. Springer Verlag, Berlin. 171–197.

Freed, M. A., R. G. Smith, and P. Sterling. 1987. Rod bipolar array in the cat retina: pattern of input from rods and GABA-accumulating amacrine cells. *J. Comp. Neurol.* 266:445–455.

Gleason, E., S. Borges, and M. Wilson. 1993. Synaptic transmission between pairs of retinal amacrine cells in culture. *J. Neurosci.* 13: 2359–2370.

Grünert, U., and P. R. Martin. 1991. Rod bipolar cells in the macaque monkey retina: immunoreactivity and connectivity. *J. Neurosci.* 11:2742–2758.

Heuser, J. E., T. S. Reese, M. J. Dennis, Y. Jan, L. Jan, and L. Evans. 1979. Synaptic vesicle exocytosis captured by quick freezing and correlated with quantal transmitter release. *J. Cell Biol.* 81:275–300.

Jack, J., S. Redman, and K. Wong. 1981. Modifications to synaptic transmission at group Ia synapses on cat spinal motoneurones by 4-aminopyridine. *J. Physiol.* 321:111–126.

Kaneko, A. 1979. Physiology of the retina. *Annu. Rev. Neurosci.* 2:169–191.

Kolb, H. 1970. Organization of the outer plexiform layer of the primate retina: electron microscopy of Golgi-impregnated cells. *Phil. Trans. Roy. Soc. (London) B*. 258:261–283.

Kolb, H. 1977. The organization of the outer plexiform layer in the retina of the cat: electron microscopic observations. *J. Neurocytol.* 6:131–153.

Kolb, H., K. A. Linberg, and S. K. Fisher. 1992. Neurons of the human retina: a Golgi study. *J. Comp. Neurol.* 318:147–187.

Korn, H., and D. Faber. 1991. Quantal analysis and synaptic efficacy in the CNS. *Trends Neurosci.* 14:439–445.

Larkman, A., K. Stratford, and J. Jack. 1991. Quantal analysis of excitatory synaptic action and depression in hippocampal slices. *Nature*. 350: 344–347.

MacLeod, D. I. A., B. Chen, and M. Crognale. 1989. Spatial organization of sensitivity regulation in rod vision. *Vision Res.* 29:965–978.

Mastronarde, D. N. 1983. Correlated firing of cat retinal ganglion cells. II. Responses of X- and Y-cells to single quantal events. *J. Neurophysiol.* 49:325–349.

Nakatani, K., T. Tamura, and K. -W. Yau. 1991. Light adaptation in retinal rods of the rabbit and two other nonprimate mammals. *J. Gen. Physiol.* 97:413–435.

Ogden, T. E. 1975. The receptor mosaic of *Aotes trivirgatus:* distribution of rods and cones. *J. Comp. Neurol.* 163:193–202.

Rao, R., and P. Sterling. 1991. Synaptic apparatus associated with transmission of a single photon event. *Soc. Neurosci.* 17:1013.

Raviola, E., and G. Raviola. 1982. Structure of the synaptic membranes in the inner plexiform layer of the retina: a freeze-fracture study in monkeys and rabbits. *J. Comp. Neurol.* 209:233–248.

Redman, S. 1990. Quantal analysis of synaptic potentials in neurons of the central nervous system. *Physiol. Rev.* 70:165–198.

Sakitt, B. 1972. Counting every quantum. *J. Physiol.* 223:131–150.

Smith, R. G., M. A. Freed, and P. Sterling. 1986. Microcircuitry of the dark-adapted cat retina: functional architecture of the rod-cone network. *J. Neurosci.* 6:3505–3517.

Steinberg, R. H., M. Reid, and P. L. Lacy. 1973. The distribution of rods and cones in the retina of the cat (*Felis domesticus*). *J. Comp. Neurol.* 148:229–248.

Sterling, P., E. Cohen, M. A. Freed, and R. G. Smith. 1987. Microcircuitry of the On-beta ganglion cell in daylight, twilight, and starlight. *Neurosci. Res.* S6:269–285.

Sterling, P., M. A. Freed, and R. G. Smith. 1988. Architecture of rod and cone circuits to the On-beta ganglion cell. *J. Neurosci.* 8:623–642.

Sterling, P., and A. B. Harkins. 1990. Ultrastructure of the cone pedicle in cat retina. *Invest. Ophthalmol. Vis. Sci.* 31:177.

Tong, G., and C. E. Jahr. 1994. Multivesicular release from excitatory synapses of cultured hippocampal neurons. *Neuron*. 12:51–59.

Trifonov, Y. A. 1968. Study of synaptic transmission between the photoreceptor and the horizontal cell using electrical stimulation of the retina. *Biofizika*. 13:809–817.

Vaney, D. I., H. M. Young, and I. C. Gynther. 1991. The rod circuit in the rabbit retina. *Vis. Neurosci.* 7:141–154.

van Trees, H. L. 1968. Detection, Estimation, and Modulation Theory. John Wiley and Sons, New York.

von Gersdorff, H., and G. Matthews. 1994. Dynamics of synaptic vesicle fusion and membrane retrieval in synaptic terminals. *Nature*. 367: 735–739.

Weibel, E. R., C. R. Taylor, and H. Hoppeler. 1991. The concept of symmorphosis: a testable hypothesis of structure-function relationship. *Proc. Natl. Acad. Sci. USA*. 88:10357–10361.

Young, H. M., and D. I. Vaney. 1991. Rod-signal interneurons in the rabbit retina: 1. Rod bipolar cells. *J. Comp. Neurol.* 310:139–153.